

# Spin-polarized transport in a lateral two-dimensional diluted magnetic semiconductor electron gas

W. Yang, Kai Chang,\* X. G. Wu, and H. Z. Zheng

NLSM, Institute of Semiconductors, Chinese Academy of Sciences, P. O. Box 912, Beijing 100083, China

The transport property of a lateral two-dimensional diluted magnetic semiconductor electron gas under a spatially periodic magnetic field is investigated theoretically. We find that the electron Fermi velocity along the modulation direction is highly spin-dependent even if the spin polarization of the carrier population is negligibly small. It turns out that this spin-polarized Fermi velocity alone can lead to a strong spin polarization of the current, which is still robust against the energy broadening effect induced by the impurity scattering.

PACS numbers: 71.70. Gm, 72.25.Dc, 72.25.Rb, 73.63.Hs

The spin of carriers in semiconductors has attracted considerable attention recently due to its great importance in the development of spintronic devices[1] and quantum computation[2]. One of the main obstacles for these potential applications is to inject highly spin-polarized carriers into semiconductors. The spin-polarized current through a diluted magnetic semiconductor (DMS) junction was predicted theoretically[3] and demonstrated experimentally by applying a strong magnetic field at low temperatures[4]. The spin polarization of the current defined as  $P_J = (J_{\uparrow} - J_{\downarrow}) / (J_{\uparrow} + J_{\downarrow})$  in semiconductors comes from two physical mechanisms. One is the contribution from the spin polarization of carrier population  $P_c = (n_e^{\uparrow} - n_e^{\downarrow}) / (n_e^{\uparrow} + n_e^{\downarrow})$ . Another important contribution is due to the difference in the spin-dependent Fermi velocity of carriers  $v_F^{\uparrow,\downarrow}$ , since the electric current depends also on the electron group velocity at the Fermi energy  $J_{\uparrow,\downarrow} = qn_e^{\uparrow,\downarrow}(E_F)v_F^{\uparrow,\downarrow}$  ( $q$  is the carrier charge). It should be emphasized that the Fermi velocity  $v_F^{\uparrow,\downarrow}$  can be engineered utilizing the spin-dependent exchange interaction, the geometric dimensionality and even the tailoring of the sample structure. Most of the previous studies focus on seeking the spin polarized current induced by the high spin polarization of carriers.

In this work we propose a structure of DMS lateral superlattice (LSL) [5, 6] and demonstrate theoretically that a strongly spin-polarized current can be generated even when the carrier spin polarization is vanishingly small. We show that in such a weakly spin-polarized system, the strong spin polarization of the current stems mainly from the difference between spin-up and spin-down Fermi velocities, instead of the spin polarization of the carriers.

As schematically shown in the inset of Fig. 1, the DMS layer is sandwiched by two nonmagnetic semiconductor (NMS) layers. Magnetic stripes with alternating magnetization directions and widths ( $L_1$  and  $L_2$ , respectively) are deposited periodically on the top of the NMS layer. The periodic magnetic field generated by the magnetic

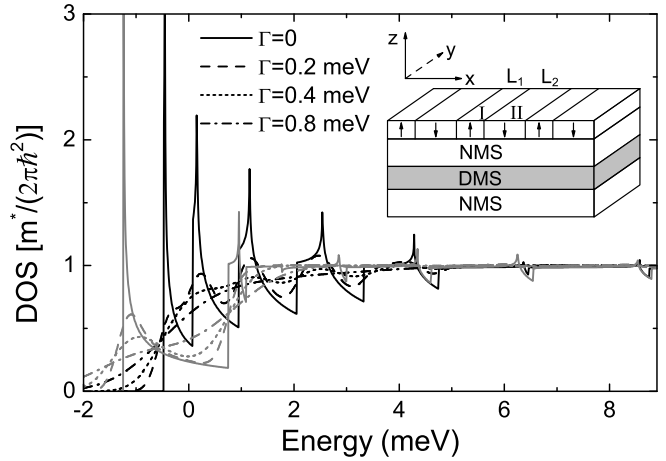


FIG. 1: The spin-up (black lines) and spin-down (gray lines) DOS for different energy broadenings  $\Gamma=0$  (solid lines), 0.2 meV (dashed lines), 0.4 meV (dotted lines), and 0.8 meV (dash-dotted lines). The inset shows schematically the DMS 2DEG sandwiched between NMS layers, with magnetic stripes deposited above.

stripes penetrates into the DMS LSL and magnetizes the Mn ions, which lead to spin splitting of the conduction electron, due to their  $s$ - $d$  exchange interaction.

The Hamiltonian for the two-dimensional electron gas in the DMS LSL reads

$$H = \frac{(\mathbf{p} + e\mathbf{A})^2}{2m^*} + H_{\text{ex}}, \quad (1)$$

here  $m^*$  is the effective mass,  $\mathbf{A} = [0, A(x), 0]$  is the vector potential for the periodic magnetic field  $\mathbf{B}(x) = B(x)\mathbf{e}_z$ , where  $B(x) = B(x + L)$  has a constant value  $B_1$  ( $B_2$ ) in region I (II). The average magnetic field  $B_{\text{av}} \equiv (B_1 L_1 + B_2 L_2)/L$  should be zero due to the sourceless nature of the magnetic field.[7, 8] This feature ensures that the Hamiltonian is periodic along the  $x$  axis.

$$H_{\text{ex}} = - \sum_i J_{s-d}(\mathbf{r} - \mathbf{R}_i) \mathbf{s} \cdot \mathbf{S}_i \quad (2)$$

describes the  $s$ - $d$  exchange interaction between conduction electrons and the  $3d^{15}$  electrons of Mn ions, where

\*Author to whom correspondence should be addressed. Electronic address:kchang@red.semi.ac.cn.

$J_{s-d}$  is the  $s$ - $d$  exchange integral,  $\mathbf{r}$  ( $\mathbf{R}_i$ ) and  $\mathbf{s}$  ( $\mathbf{S}_i$ ) are the coordinate and spin of the band electron (Mn ions), respectively. The summation runs over the lattice sites occupied by the Mn ions. Within the mean field approximation, we have  $H_{\text{ex}} = \sigma_z \Delta(x)/2$ , where  $\sigma_z$  is the  $z$  component of the Pauli matrices and  $\Delta(x) = N_0 \alpha x S_0 B_{5/2} \{g_{Mn} S \mu_B B / [k_B(T + T_0)]\}$ , with  $B_J(x)$  the Brillouin function,  $S = 5/2$  the 3d<sup>5</sup> spin of the Mn ion,  $N_0$  the number of cation sites per unit column,  $\alpha$  the  $s$ - $d$  exchange constant,  $S_0$  and  $T_0$  phenomenological parameters describing the antiferromagnetic superexchange between neighboring Mn ions.

Since  $p_y$  is a constant of motion, the electron Hamiltonian can be reduced to one-dimension effective Hamiltonian  $H_{1D} = p_x^2/(2m^*) + V_{\text{eff}}(x)$ , characterized by the periodic spin-dependent potential

$$V_{\text{eff}}(x) = V_{\text{eff}}(x + L) = \frac{1}{2m^*} [\hbar k_y + eA(x)]^2 + \sigma_z \Delta_z(x)/2.$$

Using a plane wave basis, the eigenvalues  $E_{n\sigma}(\mathbf{k})$  and eigenstates  $\psi_{n\mathbf{k}\sigma}(\mathbf{r})$  can be obtained numerically, where  $\sigma = \uparrow, \downarrow$  denotes the spin components. From the space inversion invariance of the Hamiltonian, we see that  $E_{n\sigma}(\mathbf{k})$  is invariant under the operation  $k_x \rightarrow -k_x$  or  $k_y \rightarrow -k_y$ .

The scattering effect of impurities (including the remaining parts of the  $s$ - $d$  exchange interaction not included in the mean-field approximation) can be modelled by introducing a finite broadening  $\Gamma = \hbar/\tau_c$  to the energy levels, where  $\tau_c$  is the carrier lifetime. As a result, the spin-dependent DOS per unit area is given by

$$D_\sigma(E) = \sum_n \int \frac{d^2\mathbf{k}}{(2\pi)^2} P [E - E_{n\sigma}(\mathbf{k})], \quad (3)$$

where  $P(E) = 1/(\sqrt{2\pi}\Gamma) \exp[-E^2/(2\Gamma^2)]$  is the Gaussian broadening function. The spin-dependent conductivity tensor at low temperature is given by ( $i, j = x, y$ )

$$\sigma_{ij}^\sigma = e^2 \tau \sum_n \int \frac{d^2\mathbf{k}}{(2\pi)^2} v_{n\sigma}^i(\mathbf{k}) v_{n\sigma}^j(\mathbf{k}) P [E_F - E_{n\sigma}(\mathbf{k})], \quad (4)$$

where  $\mathbf{v}_{n\sigma}(\mathbf{k}) = (1/\hbar) \nabla_{\mathbf{k}} E_{n\sigma}(\mathbf{k})$  is the group velocity and  $\tau$  is the transport relaxation time. Since the energy eigenvalue  $E_{n\sigma}(\mathbf{k})$  is an even function of  $k_x$  or  $k_y$ , all the off-diagonal conductivities vanish.

We use the following parameters for II-VI DMS  $\text{Zn}_{1-x}\text{Mn}_x\text{Se}$  in our calculation:  $m^* = 0.13m_0$  ( $m_0$  is the free electron mass),  $g_{Mn} = 2.0$ ,  $N_0\alpha = 270$  meV,  $x = 0.11$ ,  $S_0 = 0.91$ ,  $T_0 = 1.4$  K,[9, 10, 11, 12]  $T = 1$  K,  $B_1 = 0.3$  T,  $L_1 = L_2/4 = 26$  nm. The energy broadening parameter  $\Gamma$  is determined by the quality of the DMS 2DEG. It can be roughly estimated from the experimentally measured transport relaxation time  $\tau$  by assuming  $\tau_c = \tau$  (this relation holds exactly for impurity scattering by central symmetric scatterers). For non-DMS materials such as GaAs/AlGaAs 2DEG, the electron mobility can reach several tens of  $\text{m}^2/(\text{V s})$ , while for DMS 2DEG, the

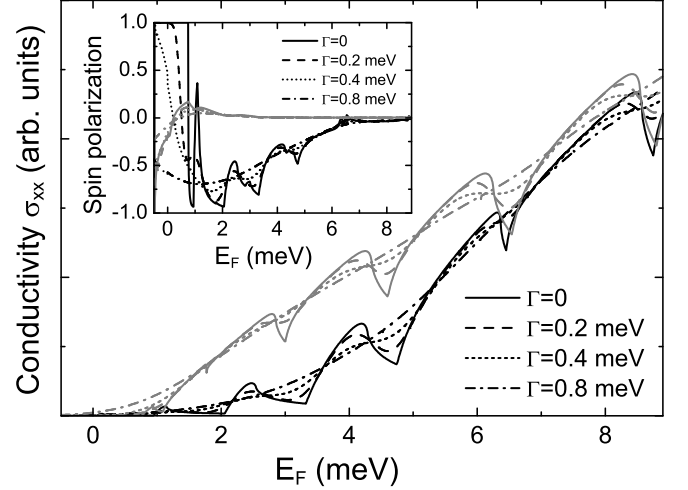


FIG. 2: Spin-up (black lines) and spin-down (gray lines) conductivities  $\sigma_{xx}$  as functions of Fermi energy. Inset shows the current polarization  $P_J$  along the  $x$  axis (black lines) and the carrier polarization  $P_c$  (gray lines). They are obtained from  $\Gamma = 0$  (solid lines), 0.2 meV (dashed lines), 0.4 meV (dotted lines), and 0.8 meV (dash-dotted lines).

mobility is decreased due to the scattering of the magnetic ions. However, high mobility II-VI DMS 2DEG has already been realized, e.g., in  $\text{HgMnTe}$  [ $\mu = 5 \text{ m}^2/(\text{V s})$ ] and  $\text{CdMnTe}$  [ $\mu = 6 \text{ m}^2/(\text{V s})$ ].[13, 14] Correspondingly, the energy broadening for  $\text{ZnMnSe}$  with mobility of the order of several  $\text{m}^2/(\text{V s})$  should be smaller than 1.0 meV. From our numerical results (to be discussed below), the energy broadening factor  $\Gamma$  is not so crucial for the spin polarization of the current.

Due to the spin-dependent effective potential  $V_{\text{eff}}(x)$ , the spin degeneracy of the electron is lifted, resulting in the spin-dependent DOS shown in Figs. 1. For vanishing energy broadening, the spin-dependent DOS shows sharp peaks (van Hove singularities) at low energy, which come from the one dimensional nature of the electron confined by  $V_{\text{eff}}(x)$ . At higher energies, the strengths of the peaks decrease, and the DOS approaches the value of a free 2DEG  $D_0 = m^*/(2\pi\hbar^2)$ , since the influence of  $V_{\text{eff}}(x)$  decreases. When finite energy broadening is taken into account, the van Hove singularities are smoothed out, even for the smallest energy broadening  $\Gamma = 0.2$  meV.

Figure 2 shows the spin-dependent conductivities  $\sigma_{xx}$  as functions of Fermi energy  $E_F$ . We see that for vanishing energy broadening,  $\sigma_{xx}$  exhibits many peaks and dips, due to the van Hove singularities in Fig. 1. With increasing energy broadening, however, these fine structures are smoothed out. The most important feature, as can be seen from the inset of Fig. 2, is the big difference between the carrier polarization  $P_c$  and current polarization  $P_J$ . The former is appreciable at low  $E_F$ , but it vanishes rapidly with increasing  $E_F$ . On the other hand, large  $P_J$  persists up to a much higher Fermi energy. In the region where  $P_c$  vanishes, this large current

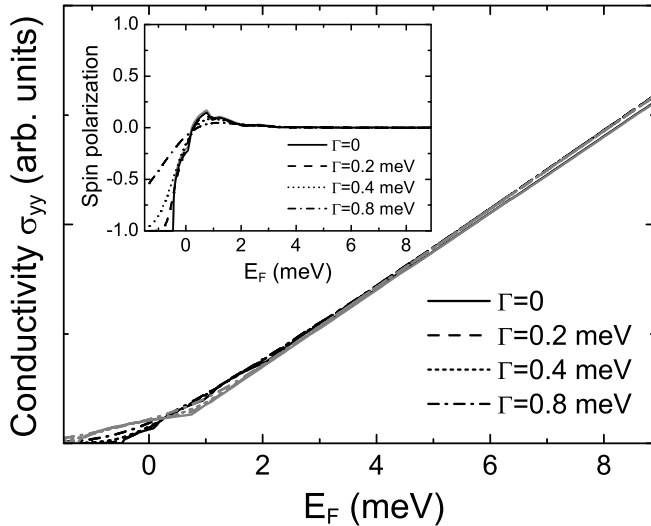


FIG. 3: Spin-up (black lines) and spin-down (gray lines) conductivities  $\sigma_{yy}$  as functions of Fermi energy. Inset: current polarization along the  $y$  axis (black lines) and carrier polarization (gray lines) as functions of Fermi energy. They are obtained from  $\Gamma=0$  (solid lines), 0.2 meV (dashed lines), 0.4 meV (dotted lines), and 0.8 meV (dash-dotted lines).

polarization stems mainly from the different Fermi velocities between electrons with different spins, instead of the polarization of the carrier itself. Further, the magnitude of  $P_J$  is nearly not affected by the increasing energy broadening, although the fine structures have been smoothed out. These interesting features demonstrate that the Fermi velocity polarization alone can also be utilized to generate a strong spin-polarized current in a weakly polarized carrier system.

Another interesting feature of this spin-polarized current is its anisotropy arising from the anisotropic struc-

ture of the DMS LSL [see the inset of Fig. 1]. In Fig. 3, we plot the spin-dependent conductivities  $\sigma_{yy}$  as functions of Fermi energy. It can be seen that  $\sigma_{yy}$  increases monotonically with increasing Fermi energy. Further, the spin polarization of  $\sigma_{yy}$  (see the inset of Fig. 3) follows closely the carrier polarization  $P_c$ . As a result, the current polarization along the  $y$  axis is always very small, except for very small Fermi energy  $E_F \lesssim 0$ . These features are quite different from those for  $\sigma_{xx}$ , due to the fact that the electron are confined by  $V_{\text{eff}}(x)$  along the  $x$  axis, while it can move freely along the  $y$  axis. When the energy broadening is increased, the fine structures of  $\sigma_{yy}$  and its spin polarization are smoothed out, similar to the case for  $\sigma_{xx}$ .

In summary, we have investigated theoretically the transport property of a 2DEG in a DMS LSL. Our numerical results demonstrate that a strongly spin-polarized current can be generated utilizing the periodic magnetic modulation in the DMS structure. The spin polarization in the carrier population could be weak, but it is still possible to generate a strongly spin-polarized current in the modulation direction. This spin polarization of the current arises from the difference between spin-up and spin-down Fermi velocities. It is still robust against the energy broadening effect induced by the impurity scattering. Our theoretical work might provide a new approach for exploiting planar spintronic devices, e.g., spin-polarized electron sources and spin filters.

### Acknowledgments

This work was partly supported by the NSFC No. 60376016 and the special fund for Major State Basic Research Project No. G001CB3095 of China.

---

[1] G. A. Prinz, Phys. Today **48**, 58 (1995); G. A. Prinz, Science **282**, 1660 (1998), and references therein.

[2] B. E. Kane, Nature (London) **393**, 133 (1998); D. Loss and D. P. DiVincenzo, Phys. Rev. A **57**, 120 (1998).

[3] J. C. Egues, Phys. Rev. Lett. **80**, 4578 (1998).

[4] R. Fiederling, M. Keim, G. Reuscher, W. Ossau, G. Schmidt, A. Waag, and L. W. Molenkamp, Nature (London) **402**, 787 (1999); Y. Ohno, D. K. Young, B. Benschoten, F. Matsukura, H. Ohno, and D. D. Awschalom, Nature (London) **402**, 790 (1999).

[5] R. R. Gerhardts, D. D. Weiss, and K. v. Klitzing, Phys. Rev. Lett. **62**, 1173 (1989); R. W. Winkler, J. P. Kotthaus, and K. Ploog, Phys. Rev. Lett. **62**, 1177 (1989); C. W. J. Beenakker, Phys. Rev. Lett. **62**, 2020 (1989); R. R. Gerhardts, Phys. Rev. B **48**, 14416 (1992).

[6] C. M. Hu, Junsaku Nitta, A. Jensen, J. B. Hansen, and Hideaki Takayanagi, Phys. Rev. B **63**, 125333 (2001).

[7] I. S. Ibrahim and F. M. Peeters, Phys. Rev. B **52**, 17321 (1995).

[8] Jirong Shi, F. M. Peeters, K. W. Edmonds, and B. L. Gallagher, Phys. Rev. B **66**, 035328 (2002).

[9] J. M. Fatah, T. Piorek, P. Harrison, T. Stirner, and W. E. Hagston, Phys. Rev. B **49**, 10341 (1994).

[10] *Physics of II-VI and I-VII Compounds, Semimagnetic Semiconductors*, edited by O. Madelung, M. Schulz, and H. Weiss Landolt-Börnstein, New Series, Group III, Vol. 17, Part b (Springer, Berlin, 1982).

[11] S. Lee M. Dobrowolska, J. K. Furdyna, H. Luo, and L. R. Ram-Mahan, Phys. Rev. B **54**, 16939 (1996).

[12] H. Jeon, J. Ding, W. Patterson, A. V. Nurmikko, W. Xie, D. C. Grillo, M. Kobayashi, and R. L. Gunshor, Appl. Phys. Lett. **59**, 3619 (1991).

[13] G. Grabecki, T. Dietl, P. Sobkowicz, J. Kossut, and W. Zawadzki, Appl. Phys. Lett. **45**, 1214 (1984).

[14] F. J. Teran, M. Potemski, D.K. Maude, Z. Wilamowski, A.K. Hassan, D. Plantier, J. Jaroszynski, T. Wojtowicz, and G. Karczewski, Physica E **17**, 335 (2003).